Analyst

Accepted Manuscript

ROYAL SOCIETY OF CHEMISTRY

www.rsc.org/analyst

Graphical Abstract

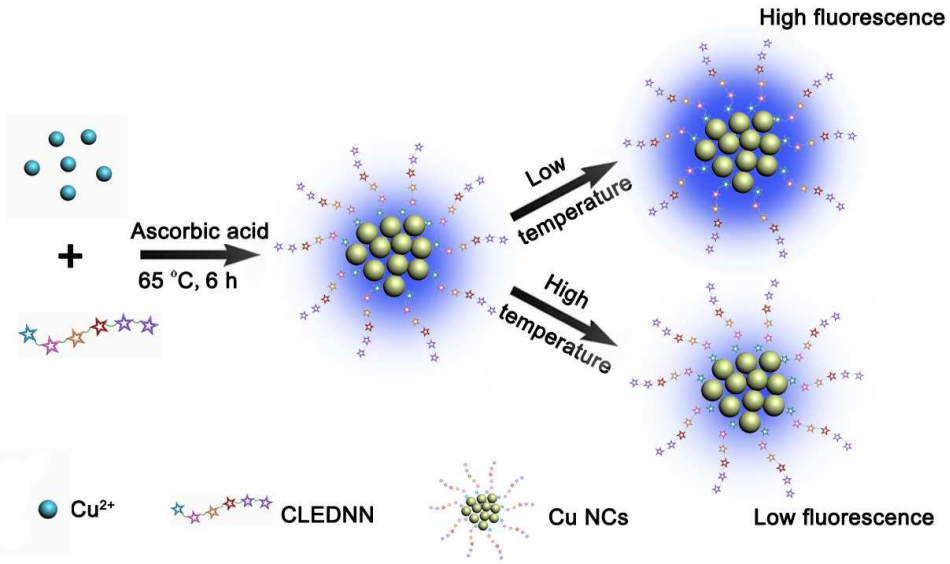

We have developed a simple and green method for synthesis of blue fluorescent peptide-templated Cu nanoclusters (NCs). The as-prepared Cu NCs display temperature dependent fluorescence and low toxicity, which can be employed as a fluorescent probe for temperature sensing and cellular imaging.

Green synthesis of peptide-templated fluorescent copper nanoclusters for temperature sensing and cellular imaging

Hong Huang, Hua Li, Ai-Jun Wang,* Shu-Xian Zhong, Ke-Ming Fang, Jiu-Ju Feng*

College of Geography and Environmental Science, College of Chemistry and Life Science, Zhejiang Normal University, Jinhua 321004, China

*Corresponding author: *E-mail:* ajwang@zjnu.cn(AJW); *E-mail:* jjfeng@zjnu.cn(JJF), Tel. /Fax: +86 579 82282269.

Abstract

A simple and green approach was developed for preparation of fluorescent Cu nanoclusters (NCs) using artificial peptide CLEDNN as a template. The as-synthesized Cu NCs exhibited high fluorescence quantum yield (7.3%) and good stability, along with excitation and temperature dependent fluorescent properties, which can be employed for temperature sensing. Further investigations demonstrated low toxicity of Cu NCs for cellular imaging.

Keywords：Peptide; Nanoclusters; Temperature sensing; Cellular imaging

Introduction

Recently, metal nanoclusters (NCs) have received tremendous attention because of

their intriguing physical, electrical, and optical properties.[1] Specifically, metallic NCs are composed of several to tens of metal atoms, which bridge the gap between atoms and metal nanoparticles.[1] They show some molecule-like properties such as discrete electronic states and strong size-dependent fluorescence over the ultraviolet to near infrared region, owing to their ultrasmall size approaching the Fermi wavelength of electrons.[2] These fluorescence features are popular for sensing and bioimaging.[3, 4] Lately, Au NCs and Ag NCs have been extensively investigated, using various templates or stabilizing agents including DNA,[5, 6] proteins,[7, 8] peptides,[9, 10] dendrimers,[11] and thiols.[12, 13] Nevertheless, Cu NCs associated investigations are still in its infancy, primarily owing to their susceptibility to oxidation and difficulty in controlling their size.

However, only a few synthetic protocols were developed for Cu NCs. Chen and coworkers prepared stable Cu_n ($n \leq 8$) NCs under argon atmosphere that is only soluble in nonpolar solvents.[14] Jia *et al.* facilely prepared Cu NCs with high fluorescence quantum yield (QY), while their stability is poor.[15] More recently, Wang's group reported protein-directed synthesis of Cu NCs,[16] involved in a very hazardous chemical of hydrazine that is toxic both to human health and environment. Therefore, it is highly pursued to develop simple and effective methods for synthesis of Cu NCs with high QY and good stability, as well as expanding their applications.

Peptides, whose composition, sequence, and length can be rationally designed through covalent chemical bonds between amino acids, have been widely used for synthesis of versatile fluorescent nanomaterials.[17-19] In this study, a simple and green

synthetic route was developed for preparation of fluorescent Cu NCs using peptide with amino acid sequence CLEDNN as a template and ascorbic acid as reductant (Scheme 1).The properties of the as-synthesized Cu NCs were investigated in some detail, and explored their potential applications as a temperature sensor and a fluorescent probe for cellular imaging.

Experimental section

Materials

Peptides with amino acid sequence CLEDNN was bought from China Peptides Co., Ltd. Copper sulfate and ascorbic acid were obtained from Sinopharm Chemical Reagent Co., Ltd. Dulbecco's modified Eagle's medium (DMEM) were obtained from Gibco BRL (USA). 3-(4,5-dimethylthia-zol-2-yl)-2,5-diphenyltetrazolium bromide (MTT) was purchased from Sigma Aldrich (USA). All the other chemicals were of analytical grade and used without further purification. Ultrapure water was used throughout the whole experiments.

Characterization

UV-vis spectroscopy (Perkin-Elmer, Lambda 950) was used to measure the optical absorption spectra. Fluorescence spectra were recorded by a fluorescence spectrophotometer (Perkin-Elmer, LS-45) equipped with a temperature control system (Thermo Electron, NESLAB RTE7). Absorption and emission measurements were

conducted in 1 cm × 1 cm quartz cuvettes. The morphology and size of Cu NCs were analyzed by transmission electron microscopy (TEM, JEM-2100F) operating at an acceleration voltage of 200 KV. The TEM specimens were prepared by placing several drops of the Cu NCs suspension onto carbon coated copper grid and then dried at room temperature. The surface groups of Cu NCs were characterized by Fourier transform infrared spectroscopy (FTIR, Thermo Electron, Nicolet 6700). For FTIR analysis, KBr crystals were used as the matrix for sample preparation. X-ray photoelectron spectra (XPS) were recorded on an X-ray photoelectron spectroscopy (Thermo Scientific, ESCALAB 250). The samples were prepared by repeatedly spotting the purified Cu NCs suspension on silicon slice and allowed to dry in an oven. Zeta potentials were measured by dynamic laser light scattering system (Malvern, ZEN3600). The fluorescence lifetime was measured on an Edinburgh FLS 920 photocounting system. Confocal images were obtained using a laser confocal scanning microscope (Leica, TCS SP5).

Preparation of Cu NCs

In a typical experiment, 50 μL of $CuSO_4$ aqueous solution (50 mM, 65 ºC) was introduced to 5 mL of the peptide solution (1.5 mg mL^{-1}, 65 ºC) under vigorous stirring. Five minutes later, 75 μL of ascorbic acid solution (100 mM, 25 ºC) was slowly added and the reaction was continued under vigorous stirring at 65 ºC for 6 h. During the reaction progress, the colorless solution gradually changed to light yellow. After the reaction completed, the solution was cooled to room temperature naturally,

purified by centrifugation at 15000 rpm for 15 min, and dialyzed against water through a dialysis membrane with a cutoff of 1000 Da for 2 days (changing the water every 8 h). The as-obtained purified Cu NCs suspension was stored at 4 °C for further use.

Quantum yield measurement

The relative QY of Cu NCs were measured in reference to quinine sulfate in 0.1 M H_2SO_4 (literature quantum yield 54% at 360 nm excitation). The same excitation wavelength and slit band widths are applied for the two samples. The formula used for QY measurements is as follows

$$QY = \frac{I}{I_R} \times \frac{A_R}{A} \times \frac{\eta^2}{\eta_R^2} \times QY_R$$

where QY is the quantum yield of the sample, I is the integral area under the fluorescence spectrum, η is the refractive index of the solvent used and A is the absorbance at the excitation wavelength. The subscript R represents the reference. To minimize reabsorption effects, absorbencies were kept under 0.1 at the excitation wavelength of 360 nm.

Effects of metal ions and NaCl concentrations

Briefly, suspensions of Cu NCs (60 μg mL^{-1}, 10 μL) were added separately into 400 μL phosphate buffer solution (25 mM, pH 7.4) containing different common metal ions with a final concentration of 50 μM and mixed thoroughly. The fluorescence spectra were recorded after reaction for 30 min. The effects of NaCl concentrations

were examined in a similar way, in which NaCl solutions with different concentrations (50, 100, 150, and 200 mM) were used instead of phosphate solutions. The experiments were performed at room temperature.

Temperature sensing

Typically, 1 mL Cu NCs suspension (60 μg mL^{-1}) was introduced into a quartz cuvette. After setting the temperature (increasing the temperature from 10 to 55 ºC), we waited for 10 min before recording the corresponding fluorescence spectra.

In vitro toxicity assay

HeLa cells and human embryonic kidney (HEK) 293 cells were harvested (the cell density was adjusted to 10^5 cells mL^{-1}) and seeded in a 96-well plate (90 μL $well^{-1}$) overnight, followed by the introduction of Cu NCs suspension with different concentration (10, 25, 50, 75, and 100 μg mL^{-1}). Five replicate samples were prepared for each concentration. The cells were cultivated for 24 h and then 20 μL of MTT solution (1 mg mL^{-1}) was put into each cell well. After incubation for another 4 h, the culture medium was discarded, followed by the addition of 150 μL dimethyl sulphoxide (DMSO). The resulting mixture was shaken for 15 min in dark at room temperature. The optical density (OD) of the mixture was measured at 570 nm with a thermo multiskan spectrum microplate spectrophotometer. The cells cultured with the pure medium were used as a control. The cell viability was estimated according to the following equation:

$$\text{Cell viability (\%)} = OD_{\text{treated}} / OD_{\text{control}} \times 100\%$$

where OD_{control} was obtained in the absence of Cu NCs, while OD_{treated} was obtained with Cu NCs.

Cell imaging

HeLa cells were cultured in DMEM containing 10% fetal bovine serum and 100 μg mL^{-1} penicillin/streptomycin in a humidified incubator at 37 °C and 5% CO_2. The as-synthesized Cu NCs solution was injected into the well of a chamber slide, with the final concentration of 100 μg mL^{-1}. After incubation of 24 h, the cells were extensively washed with phosphate buffered saline, and recorded the corresponding fluorescence images with UV light excitation (λ = 355 nm).

Results and discussion

Fluorescent Cu NCs were synthesized in one step by reducing copper salt with ascorbic acid in the presence of peptide CLEDNN at 65 °C for 6 h. The as-obtained Cu NCs suspension is light yellow in visible light (Figure 1A) and emits strong blue fluorescence under 365 nm UV light (Figure 1B). In contrast, nearly no fluorescence is observed for the reactants, showing the formation of fluorescent Cu NCs. The fluorescent Cu NCs show the maximum excitation and emission peaks at 373 and 454 nm, respectively (Figure 1C). Impressively, no absorption peak is detected within the wavelength range of 300~600 nm for the absorption spectrum of Cu NCs (Figure 1C), which is remarkably different from that of Cu nanoparticles with the characteristic

surface Plasmon resonance absorption peak at 507 nm.[12] The result indicates that Cu NCs have a size below 5 nm,[20] as strongly supported by the following TEM measurements.

The peptide-Cu NCs display excitation dependent fluorescent emission spectra, similar to lysozyme-Cu NCs prepared in the literature.[21] As illustrated in Figure S1, the emission peak is gradually red shifted from 452 to 523 nm by varying the excitation wavelength from 360 to 470 nm with 10 nm increment, accompanied by the decrease of the fluorescence intensity. The QY of Cu NCs is calculated to be 7.3%, using quinine sulfate (54% in 0.1 M H_2SO_4) as a reference. This value is smaller than that of penicillamine-Cu NCs (16.6%),[15] but larger than that of BSA-Cu NCs (4.1%) in the literature.[16]

Transmission electron microscopy (TEM) image shows that well-dispersed Cu NCs have spherical nanostructure and narrow size distribution (Figure 2A). By measuring 100 random clusters, the average diameter of Cu NCs is determined to be 1.7 ± 0.4 nm (Figure 2B). This value is very close to DNA-hosted Cu NCs.[22] High-resolution TEM (HRTEM) image reveals an inter-fringe spacing of 0.206 nm for Cu NCs (inset in Figure 2A), which was consistent with the (111) crystal planes of metallic Cu.[23]

X-ray photoelectron spectroscopy (XPS) analysis reveals the coexistence of C, O, N, S, and Cu elements in Cu NCs (Figure S2). As displayed in Figure 3A, there are two strong peaks emerged at 932.3 and 952.3 eV, corresponding to Cu $2p_{3/2}$ and Cu $2p_{1/2}$, respectively, which are characteristic peaks of Cu^0. The lack of satellite peak at around 942 eV means the absence of Cu^{2+} in the present system, which is different

from Cu NCs prepared by electrochemical method.[24] Additionally, it is worthwhile mentioning that the binding energy of Cu $2p_{3/2}$ of Cu^0 is only 0.1 eV apart from that of Cu^+. Therefore, Cu atoms in Cu NCs might have two valence states, i.e., 0 and/or +1.

Fourier transform infrared (FTIR) spectra are provided for the peptide CLEDNN and Cu NCs (Figure 3B). The disappearance of the S-H stretching vibration band (2564 cm^{-1}) of the peptide from the surface of Cu NCs indicates the formation of Cu-S bonds between the peptide and Cu NCs. Meanwhile, the zeta potential of Cu NCs was measured to be –14.5 mV (Figure S3), which is attributed to the existence of hydroxyl and carboxyl groups on the surface of Cu NCs, as displayed by the FTIR spectrum of Cu NCs, revealing the characteristic absorption peaks of O-H and C=O groups at 3420 and 1665 cm^{-1}, respectively.

Furthermore, the stability of Cu NCs was investigated under different conditions. The fluorescence intensity of Cu NCs remains unchanged in the presence of NaCl solution with different concentrations (up to 200 mM), implying good stability of Cu NCs under high ionic strength environment (Figure 4A). Meanwhile, common metal ions such as Hg^{2+}, Cd^{2+}, Zn^{2+}, Fe^{3+}, Ba^{2+}, Ca^{2+}, Co^{2+}, Pb^{2+}, Ag^{+}, Ni^{2+}, and Cr^{3+} (50 μM) show negligible interference on the fluorescence intensity (Figure 4B). Besides, varying the pH values from 3.0 to 9.0 yields no influence on the corresponding fluorescence spectra. It indicates that Cu NCs are insensitive to the pH values in the present system (Figure 4C). This observation is distinguished from Cu NCs reported by Huang's group.[23] After storage of 1 month in air at room temperature, no any precipitate, flocculation, or the loss of fluorescence is observed for Cu NCs (Figure

4D). All these observations manifest the improved stability of Cu NCs, combined with their small size and high fluorescence, making them very promising for cellular imaging.

Most importantly, the fluorescence of Cu NCs displays a temperature dependent feature. As shown in Figure 5A, increasing the temperature from 10 to 55 ºC causes a monotonous decrease of the fluorescence intensity. The fluorescence intensity drops to 62% of its initial value by increasing the temperature from 10 to 55 ºC (Figure 5B), with the sensitivity of –0.83% ºC $^{-1}$, which is comparable with that of polymer dots in the literature.[25] The decrease of fluorescence intensity at high temperature is probably due to the enhancement of the nonradiative decay.[26, 27] This assumption is verified by the fluorescence lifetime measurements of Cu NCs at different temperature. The corresponding fluorescence lifetime is decreased from 5.38 ns at 10 ºC to 2.26 ns at 55 ºC (Figure 5C). More importantly, the reversible process can be readily repeated 6 cycles with negligible fatigue in the temperature window (Figure 5D), which provides the great potential application of Cu NCs in the construction of temperature sensitive devices.

As known, Cu is an essential trace element for human health, and Cu NCs are synthesized herein by a green method at lower temperature in comparison with that reported by Fernandez-Ujados,[28] without any toxic agent or organic solvent involved.[29] Thus, we speculate that Cu NCs have low cytotoxicity. The cytotoxicity of Cu NCs was further checked by measuring the relative viability of HeLa cells, a human cervical cancer cell line, and HEK 293 cells, a normal cell line, when the cells

were exposed to Cu NCs with different concentrations by a standard MTT assay. As depicted in Figure 6, there is no reduction in the cell viability of both cell lines after incubation of 24 h with high concentrations of Cu NCs even up to 100 μg mL^{-1}, suggesting low cytotoxicity of Cu NCs.

We used Cu NCs as a fluorescent probe for imaging HeLa cells, which were cultured in an appropriate culture medium containing 100 μg mL^{-1} Cu NCs, and the fluorescence microscope images were taken with an excitation wavelength of 355 nm. After incubation of 24 h, a remarkably blue fluorescence is observed in the cell membrane and cytoplasmic area, whereas the fluorescence in the cell nucleus is very weak (Figure 7). These results imply that nearly no Cu NCs enter the inner nuclei, which would avoid genetic disruption, and thereby confirm that Cu NCs can serve as an attractive probe in bio-imaging.

Conclusions

In summary, this study provides a simple and green method for preparing fluorescent Cu NCs using the peptide CLEDNN as a template. The as-prepared Cu NCs exhibit good stability, high QY, low cytotoxicity, and thermoresponsive fluorescence with good reversibility, which can be used as a fluorescent probe for cellular imaging and temperature sensing. Further investigations of its potential applications in mapping intracellular temperature are still in progress. In view of the facile and green synthesis route and fascinating luminescent features, the as-synthesized Cu NCs hold great promise for imaging, sensing, catalysis, and other

applications.

Acknowledgments

This work was financially supported by National Natural Science Foundation of China (No. 21475118, 21175118, and 21275130), and Zhejiang province university young academic leaders of academic climbing project (No. pd2013055).

Reference

1. R. Jin, *Nanoscale*, 2010, **2**, 343-362.
2. Y. Lu and W. Chen, *Chem. Soc. Rev.*, 2012, **41**, 3594-3623.
3. L. Shang, S. Dong and G. U. Nienhaus, *Nano Today*, 2011, **6**, 401-418.
4. Z. Luo, K. Zheng and J. Xie, *Chem. Commun.*, 2014, **50**, 5143-5155.
5. X. Yang, L. Gan, L. Han, E. Wang and J. Wang, *Angew. Chem.*, 2013, **125**, 2076-2080.
6. G. Wang, Y. Zhu, L. Chen, L. Wang and X. Zhang, *Analyst*, 2014, **139**, 165-169.
7. J. Qiao, X. Mu, L. Qi, J. Deng and L. Mao, *Chem. Commun.*, 2013, **49**, 8030-8032.
8. M. Zhuang, C. Ding, A. Zhu and Y. Tian, *Anal. Chem.*, 2014, **86**, 1829-1836.
9. Y. Cui, Y. Wang, R. Liu, Z. Sun, Y. Wei, Y. Zhao and X. Gao, *ACS Nano*, 2011, **5**, 8684-8689.
10. Y. Gu, Q. Wen, Y. Kuang, L. Tang and J. Jiang, *RSC Adv.*, 2014, **4**, 13753-13756.
11. J. Zheng, J. T. Petty and R. M. Dickson, *J. Am. Chem. Soc.*, 2003, **125**,

7780-7781.

12. L. Shang, F. Stockmar, N. Azadfar and G. U. Nienhaus, *Angew. Chem. Int. Ed.*, 2013, **52**, 11154-11157.

13. L. Shang, S. Brandholt, F. Stockmar, V. Trouillet, M. Bruns and G. U. Nienhaus, *Small*, 2012, **8**, 661-665.

14. W. Wei, Y. Lu, W. Chen and S. Chen, *J. Am. Chem. Soc.*, 2011, **133**, 2060-2063.

15. X. Jia, X. Yang, J. Li, D. Li and E. Wang, *Chem. Commun.*, 2014, **50**, 237-239.

16. C. Wang, C. Wang, L. Xu, H. Cheng, Q. Lin and C. Zhang, *Nanoscale*, 2014, **6**, 1775-1781.

17. Y. Wang, Y. Cui, Y. Zhao, R. Liu, Z. Sun, W. Li and X. Gao, *Chem. Commun.*, 2012, **48**, 871-873.

18. Y. Wang, Y. Cui, R. Liu, Y. Wei, X. Jiang, H. Zhu, L. Gao, Y. Zhao, Z. Chai and X. Gao, *Chem. Commun.*, 2013, **49**, 10724-10726.

19. J.-J. Feng, H. Huang, D.-L. Zhou, L.-Y. Cai, Q.-Q. Tu and A.-J. Wang, *J. Mater. Chem. C*, 2013, **1**, 4720-4725.

20. X. Jia, J. Li and E. Wang, *Small*, 2013, **9**, 3873-3879.

21. R. Ghosh, A. K. Sahoo, S. S. Ghosh, A. Paul and A. Chattopadhyay, *ACS Appl. Mater. Interfaces*, 2014, **6**, 3822-3828.

22. X. Jia, J. Li, L. Han, J. Ren, X. Yang and E. Wang, *ACS Nano*, 2012, **6**, 3311-3317.

23. W. Wang, F. Leng, L. Zhan, Y. Chang, X. X. Yang, J. Lan and C. Z. Huang, *Analyst*, 2014, **139**, 2990-2993.

24. N. Vilar-Vidal, M. C. Blanco, M. A. López-Quintela, J. Rivas and C. Serra, *J. Phys. Chem. C*, 2010, **114**, 15924-15930.

25. F. Ye, C. Wu, Y. Jin, Y.-H. Chan, X. Zhang and D. T. Chiu, *J. Am. Chem. Soc.*, 2011, **133**, 8146-8149.

26. R. Liang, R. Tian, W. Shi, Z. Liu, D. Yan, M. Wei, D. G. Evans and X. Duan, *Chem. Commun.*, 2013, **49**, 969-971.

27. X. Yuan, T. J. Yeow, Q. Zhang, J. Y. Lee and J. Xie, *Nanoscale*, 2012, **4**, 1968-1971.

28. F.-U. Mónica, T.-A. Laura, M. C.-F. José, P. Rosario and S.-M. Alfredo, *Nanotechnology*, 2013, **24**, 495601.

29. H. Kawasaki, Y. Kosaka, Y. Myoujin, T. Narushima, T. Yonezawa and R. Arakawa, *Chem. Commun.*, 2011, **47**, 7740-7742.

Captions

Scheme 1 Schematic illustration of the formation mechanism of Cu NCs with temperature dependent fluorescence.

Figure 1 Photographs of Cu NCs under visible light (A) and UV light at 365 nm (B). UV-vis absorption (a) and fluorescence (b: excitation spectrum; c: emission spectrum) spectra of Cu NCs (C).

Figure 2 TEM image of Cu NCs (A) and the corresponding size-distribution histogram (B). Inset shows the associated HRTEM image.

Figure 3 (A) High-resolution Cu 2p XPS spectrum of Cu NCs. (B) FTIR spectra of the peptide CLEDNN and Cu NCs.

Figure 4 Effects of NaCl concentrations (A), common metal ions (B), pH values (C), and storage time (D) on the fluorescence intensity of Cu NCs.

Figure 5 (A) Fluorescence of Cu NCs in response to temperature change in the range of 10~55 ºC. The fluorescence spectra were normalized to maximum intensity for clarity. (B) The relationship between the fluorescence intensity change and the temperature. (C) The fluorescence response of six consecutive cycles between 10 and

55 ºC. (D) Fluorescence decay traces of Cu NCs recorded at 10 and 55 ºC.

Figure 6 Viability of HeLa cells (the gray bars) and HEK 293 cells (the red bars) after incubation of 24 h with different concentrations of Cu NCs solutions.

Figure 7 Images of Cu NCs incubated HeLa cells obtained under bright field (A) and excitation wavelength of 355 nm (B). Scale bar: 25 μM.

Figures

Scheme 1

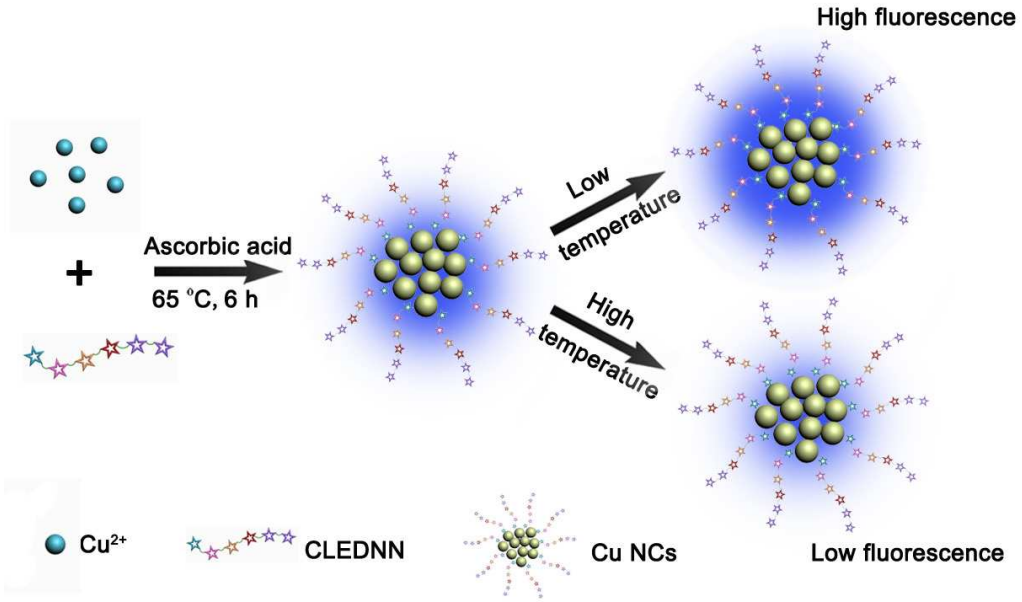

Figure 1

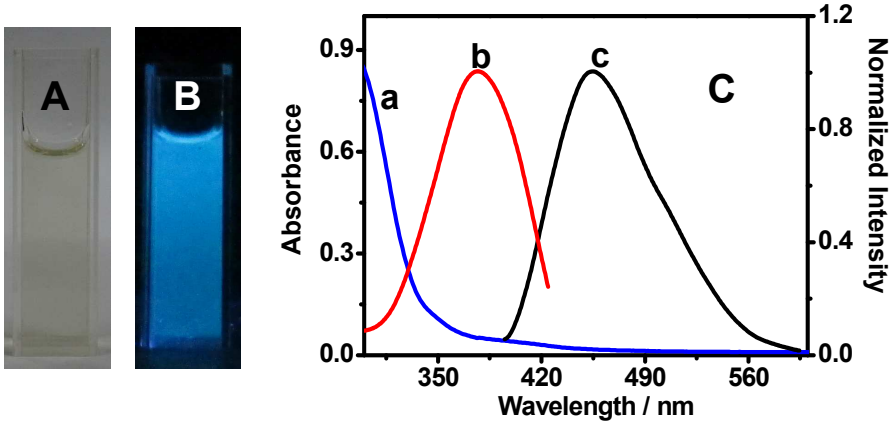

Figure 2

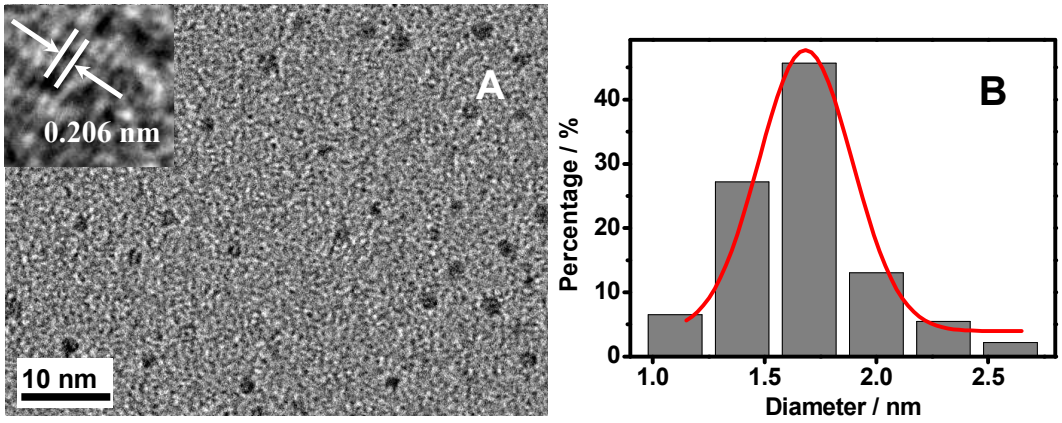

Figure 3

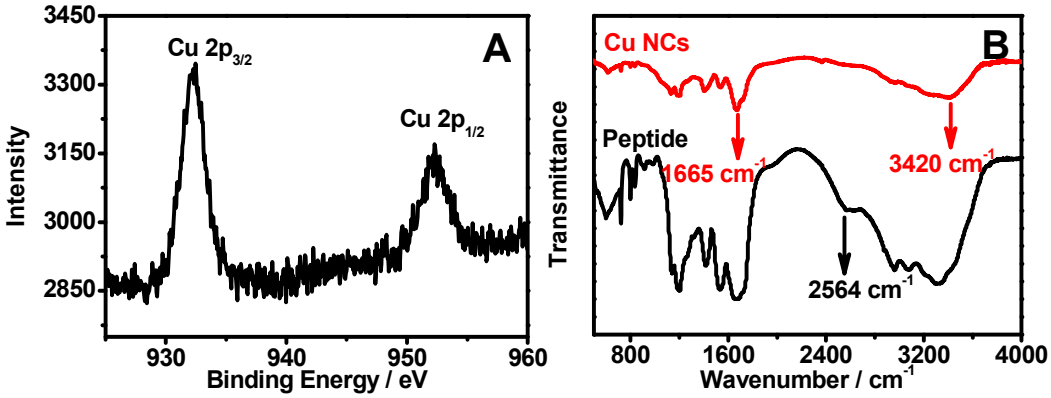

Figure 4

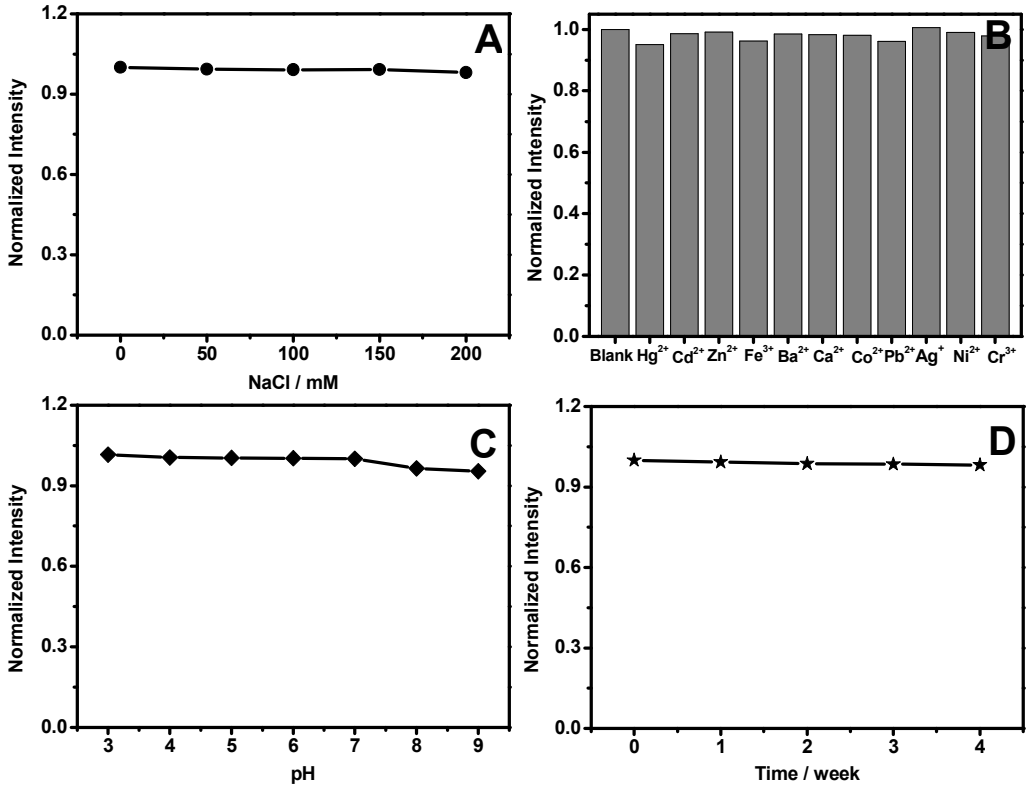

Figure 5

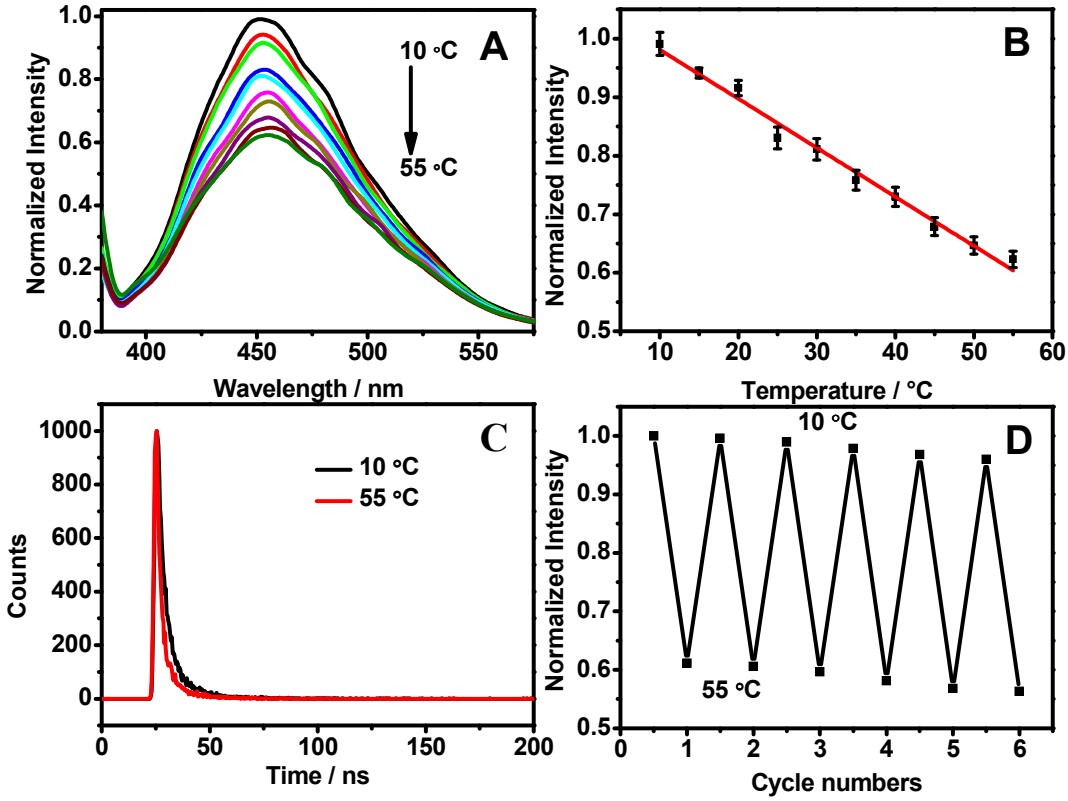

Figure 6

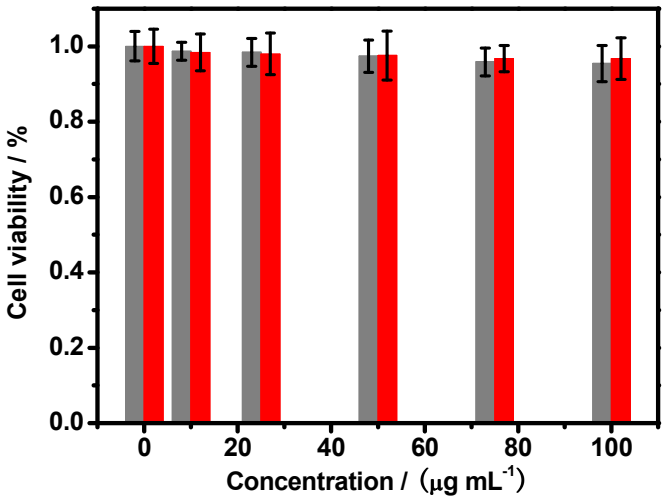

Figure 7